3. Assumptions for Mars RF Link Design

High-rate communications from Mars has significant but manageable challenges during the timeline 2020 to 2030. MRO sends data on X-band at rates as high as 5.3 Mbps. MRO could have been designed to send data at much higher rates than 5.3 Mbps over most Mars-Earth distances were it not for bandwidth limitations at X-band (ref. 3–1).

The bandwidth issue is less severe at Ka-band. The deep space allocation for Ka-band is 500 MHz, compared with 50 MHz at X-band. This section discusses the various assumptions and challenges foreseen for a high rate Ka-band downlink. These assumptions and challenges include spacecraft constraints, ground station configuration, weather and atmospheric implications, solar conjunction, spectrum constraints, and the extreme variation in Earth-Mars distance.

3.1 Spacecraft Constraints

High-rate communications from Mars requires developing RF technology capability with high availability, reliability, and increased bandwidth. The high rate will result in the use of large antennas along with high-power transmitters. The requirement for generating a specific effective EIRP is a function of a trade between the Earth station G/T (antenna gain to operating temperature ratio) and the spacecraft power/gain parameters. Some of the spacecraft assumptions to be used for design and analysis, based on the ongoing technology research discussed in chapters 5 and 6, are the following:

- Power amplifier RF output levels range from 0.2 to 2.5Kw
- Antenna diameters range from 4 to 25 m. Antennas below 12 m are assumed to be pointed with the spacecraft ACS, while larger antennas would require a fine-pointing mechanism.
- A worst-case pointing error loss of 1 dB and a worst-case pointing ability of 14 mdeg (coarse pointing) are required. This assumes the high-gain antenna (HGA) pointing to Earth is body mounted and depends on the spacecraft ACS for antenna pointing accuracy.
- The spacecraft antenna for the link to Earth always points at Earth, implying that the antenna for proximity communications will require a gimbaled mechanism. Proximity communications and antennas are not covered here and will need to be visited in the future.

Other issues and concerns, addressed in chapters 5 and 6, include the availability of

- space-qualifiable RF components operating at high power levels with low mass and good power conversion efficiency
- Ka-band antennas with good efficiency
- deployment mechanisms for large antennas

3.2 Ground Network

The ground network assumed for the Mars-to-Earth communications links is the future DSN ground network array, composed of multiple 12-m antennas, along with the associated electronics and control systems, at each of three sites. For comparison, this section also provides the capabilities of the existing (2005) DSN with its 34- and 70-m antennas.

The DSN plans to develop an initial array with 12 elements for demonstration by midcalendar year 2007 and will operationally deploy the array at each of the DSN sites with as many elements as is required starting in mid-2010. With respect to supporting the Mars relay, however, a trade space will be investigated in which the DSN array at three sites is assumed for this service, starting around the year 2020.

The telecommunications link between the Earth and spacecraft engaged in solar system exploration at Mars includes the DSN. This network currently consists of large antennas spaced approximately equally in longitude around the Earth (ref. 3–2). The current DSN has a few large antennas at each of three longitudes (sites): Goldstone, California, U.S.A.; Madrid, Spain; and Canberra, Australia. Each site includes one 70-m Cassegrain antenna, one 34-m high-efficiency (HEF) antenna, and from one to three 34-m beam-waveguide (BWG) antennas.

Table 3–1 provides the major downlink (receive) performance parameters at X-band and Ka-band for the existing 34-m antennas. The HEF stations listed in the table are DSS–15 (Goldstone), DSS–45 (Canberra), and DSS–65 (Madrid). The BWG stations that have both X-band and Ka-band receive capability are DSS–25 and DSS–26 (Goldstone), DSS–34 (Canberra), and DSS–55 (Madrid).

TABLE 3–1.—RECEIVE PERFORMANCE PARAMETERS FOR CURRENT 34-m DSN ANTENNAS

Parameter	X-band value	Ka-band value
HEF stations, frequency range (MHz)	8400 to 8500	
BWG stations, frequency range (MHz)	8400 to 8500	31 800 to 32 300
HEF stations, gain, diplexed value (no atmosphere included), dB	68.3	
BWG stations, gain, diplexed value (no atmosphere included), dB	68.3	79.1
HEF stations, system temperature, diplexed, K	28.9 (Goldstone) 29.3 (Canberra) 29.2 (Madrid)	
BWG stations, system temperature, diplexed, K (values at each site depend on polarization)	17.9 or 18.8 (DSS–26) 19.0 or 19.4 (DSS–34) 19.9 or 20.3 (DSS–55)	21.9 or 23.3 (DSS–26) 21.4 or 21.6 (DSS–34) 22.3 or 23.3 (DSS–55)
HEF antenna polarization	Dual circular (receive same as or opposite from transmit polarization)	
BWG antenna polarization	Dual circular (available simultaneously)	Dual circular (DSS–25 is RCP only)

3.2.1 DSN-Array Downlink Capability

Future missions, including the Mars relay scenario defined in section 2, require improvements in the telecommunications link with Earth by a factor of up to 1000. The DSN plans (refs. 3–3 to 3–5) to achieve this increase with an array of 12-m antennas. The DSN array will be at a single site per longitude. For the purpose of this study a maximum 180-element array is assumed for a link from Mars to Earth. Figure 3–1 shows an artist's conception of the deployed array.

The architecture for the DSN array consists of a single cluster of closely spaced antennas at each site (ref. 3–6). For an array with telecommunications as its primary purpose, tightly clustered placement of the individual elements is most efficient to improve the ability of the array combiner software to phase up on the weak sources.

The array will comprise antennas, electronics, signal combiner, control and analysis software, and the infrastructure, including the control buildings, roads, fences, security system, and intra-array communications system. Table 3–2 shows the major X-band and Ka-band characteristics of the array.

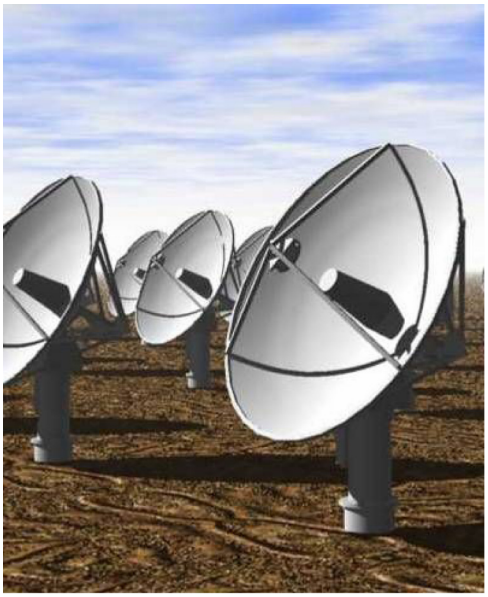

Figure 3–1.—An artist's conception of the DSN-array.

TABLE 3–2.—DSN-ARRAY CHARACTERISTICS AT X-BAND AND Ka-BAND

Requirement	X-band	Ka-band
Element size (diam., m)	12	12
Antenna element efficiency, percent	65	65
Array zenith noise temperature, average clear (50 percent) weather, K	20	40
Polarization	Dual circular	Dual circular
Array beams per cluster	Up to 16	Up to 16

3.2.2 Array Operations Concept

The paradigm currently used by the DSN consists of providing a set of services via the 34- or 70-m stations or array of these large antennas at a single site or across sites (e.g., Goldstone-Canberra), with the modeled link performance being largely fixed except for elevation angle. Project spacecraft telecommunications system engineers design their systems to use these fixed services.

The planned use of DSN array is complementary to the assumptions of the Space Communications Architecture Working Group (SCAWG's) scenario. The project's system and mission planners would request a particular minimum aperture/temperature and system availability. This allows the array scheduling system to allocate only the number of antennas required to meet the performance required in addition to the marginal extra antennas to meet the availability requirement. In this way, the number of multiple missions to be supported can be maximized. The projects and the DSN can negotiate performance as a function of cost and availability.

3.3 Atmospherics and Weather

On the basis of a free-space link budget, assuming equal antennas (diameter and efficiency) and equal transmitted power, Ka-band downlink communications has an advantage of about 11 dB as compared to X-band. This section describes how this Ka-band advantage is whittled away by the increases in system noise temperature and its variability, both of which are larger at Ka-band. It also suggests that data rate optimization techniques can mitigate some of the effects. The trades involve not only data volume per pass but also link reliability through the pass.

The principal sources of atmospheric attenuation and noise temperature weather effects are oxygen, water vapor, clouds, and rain (ref. 3–2). The noise temperature is completely determined as a function of attenuation, and higher atmospheric attenuation produces a higher noise temperature. The governing equations from (ref. 3–2) are shown in appendix 3A. Atmospheric effects generally increase with increasing frequency. Ka-band effects are larger than X-band effects, which are larger than S-band effects. The average attenuation and its variability both increase with decreasing elevation angle.

Under realistic channel conditions, the 11-dB Ka-band advantage over X-band is reduced. This is primarily because of a greater magnitude and variability at Ka-band than at X-band in the system temperature associated with atmospheric moisture. Greater Ka-band signal attenuation through the atmosphere also contributes to the smaller than expected downlink performance difference between the two frequencies. As a function of the specific transmission strategy used to combat terrestrial weather conditions, the actual Ka-band advantage can be anywhere from 5 to 7 dB.

Atmospheric noise temperature and attenuation affect link reliability since an outage occurs whenever an elevated noise temperature and increased attenuation cause the SNR to fall below the threshold.

Tables 3–3 and 3–4 show Ka-band and X-band noise temperatures and atmospheric attenuations (refs. 3–2, 3–7, and 3–8). The tables are organized to show atmospheric effects in terms of "90 percent weather," "95 percent weather," and "99 percent weather." These terms mean that the noise temperature and attenuation exceed the tabulated values only 10, 5, or 1 percent of the time, respectively.

TABLE 3–3.—Ka-BAND ZENITH NOISE TEMPERATURE AND ATMOSPHERIC ATTENUATION

Cumulative distribution	Complex	Noise temperature, K					Atmospheric attenuation, dB				
		Avg.	Min.	Month	Max.	Month	Avg.	Min.	Month	Max.	Month
90%	Canberra	24.6	17.6	July	37.2	Feb.	0.404	0.285	July	0.624	Feb.
	Madrid	24.5	17.2	July	34.0	Oct.	0.401	0.279	July	0.568	Oct.
	Goldstone	15.1	11.7	Apr.	18.4	July	0.243	0.188	Apr.	0.298	July
95%	Canberra	36.0	24.0	July	52.9	Feb.	0.600	0.391	July	0.913	Feb.
	Madrid	37.3	18.5	July	58.4	Jan.	0.624	0.298	July	1.021	Jan.
	Goldstone	18.1	12.7	Apr.	23.2	Jan.	0.291	0.202	Apr.	0.377	Jan.
99%	Canberra	75.4	44.1	July	110.4	Feb.	1.364	0.744	July	2.181	Feb.
	Madrid	68.7	28.1	July	99.0	Oct.	1.225	0.460	July	1.896	Oct.
	Goldstone	32.7	21.3	Apr.	50.4	Jan.	0.541	0.344	Apr.	0.863	Jan.

TABLE 3–4.—X-BAND ZENITH NOISE TEMPERATURE AND ATMOSPHERIC ATTENUATION

Cumulative distribution	Complex	Noise temperature, K					Atmospheric attenuation, dB				
		Avg.	Min.	Month	Max.	Month	Avg.	Min.	Month	Max.	Month
90%	Canberra	3.53	3.05	July	4.40	Feb.	0.056	0.048	July	0.069	Feb.
	Madrid	3.45	2.95	July	4.11	Oct.	0.054	0.046	July	0.065	Oct.
	Goldstone	2.72	2.48	Apr.	2.95	July	0.043	0.039	Apr.	0.046	July
95%	Canberra	4.31	3.48	July	5.48	Feb.	0.068	0.055	July	0.086	Feb.
	Madrid	4.34	3.03	July	5.98	Jan.	0.068	0.048	July	0.091	Jan.
	Goldstone	2.92	2.55	Apr.	3.28	Jan.	0.046	0.040	Apr.	0.051	Jan.
99%	Canberra	7.04	4.87	July	9.47	Feb.	0.111	0.076	July	0.150	Feb.
	Madrid	6.51	3.70	July	8.61	Oct.	0.102	0.058	July	0.136	Oct.
	Goldstone	3.94	3.15	Apr.	5.17	Jan.	0.062	0.049	Apr.	0.081	Jan.

The tables provide year-average values (labeled "avg."), as well as values (labeled "min.") for the best month and (labeled "max.") for the worst month for weather at the particular site. The 90 percent year-average system temperature (24.6 K) and attenuation for Canberra (0.404 dB) are highlighted in red; they appear in the calculation example in appendix 3A.

The DSN employs receivers with internal noise temperatures as low as 25 K. A typical DSN link is operated at 90 to 95 percent link availability for S-band or X-band communications, with average temperature increases a small fraction of the 25 K (table 3–4: 2 to 4 K average and

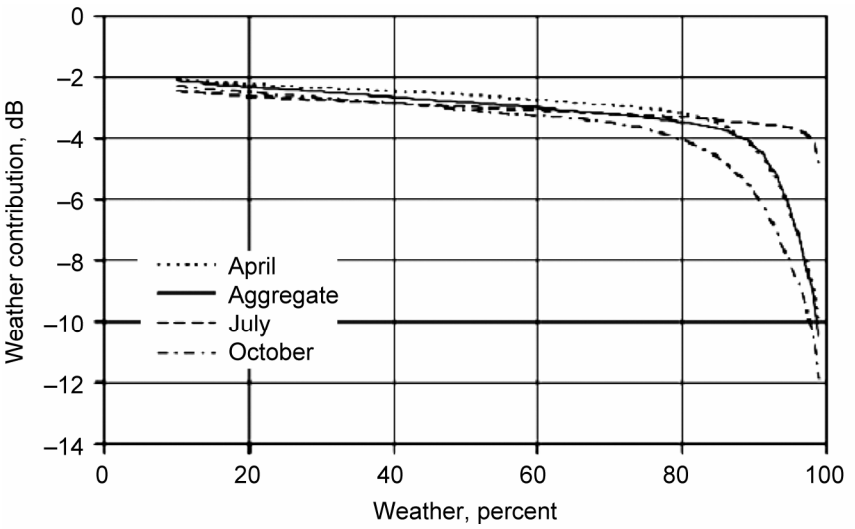

Figure 3–2.—Ka-band downlink degradation as a function of percent weather. Weather contributions to Ka-band G/T at 30° elevation versus percent weather for different atmospheric noise temperature distributions, 34-m BWG antenna, Madrid.

worst case of 6 K). Going to Ka-band results in temperatures generally higher than the receiver temperature itself (table 3–3: 15 to 37 K average and worst case of 58 K).

The main challenge Ka-band presents in determining an appropriate link margin is the large noise temperature variability due to weather. Figure 3–2 indicates the range of variability on the Ka-band link at a 30° elevation angle at Madrid. For 90 percent cumulative distribution (CD), the difference between the worst month (October) and the best month (July) is 3 dB. For 95 percent CD, the difference is 5 dB. The differences at a given CD become larger as the elevation angle decreases below 30°.

There are several methods (refs. 3–9 and 3–10) of "optimizing" the profile of data rate as a function of time in a pass to maximize the total data volume. These methods are compared against the standard practice requiring a single reliability (e.g., 90 percent weather) and setting a single data rate for the entire pass to meet the required reliability at minimum elevation angle. Standard practice also includes a 3 dB margin to cover all factors other than weather variability.

Figure 3–3 (ref. 3–10) shows results for one such kind of optimization, the continuously variable data rate (CVDR). The vertical axis is data volume returned per pass, normalized for a particular EIRP that is the same for Ka-band and X-band. The horizontal lines at 52.2 dB for Ka-band and 46.2 dB at X-band are for downlinks at a single data rate and 90 percent CD.

Year-average or specific-month results for Ka-band and X-band depend on the site and the minimum elevation angle during the scheduled pass. Figure 3–3 is for year-average at Madrid with a minimum elevation angle of 10°. The two curves show the difference in data volumes for X-band and Ka-band return links and their variability with respect to link availability. With similarly powered X-band and Ka-band transmitters and CVDR, the normalized data volume of Ka-band link at 80 percent link availability is 57.4 dB, while the volume of X-band at 90 percent availability is 52.1 dB, showing an advantage for Ka-band of about 5 dB.

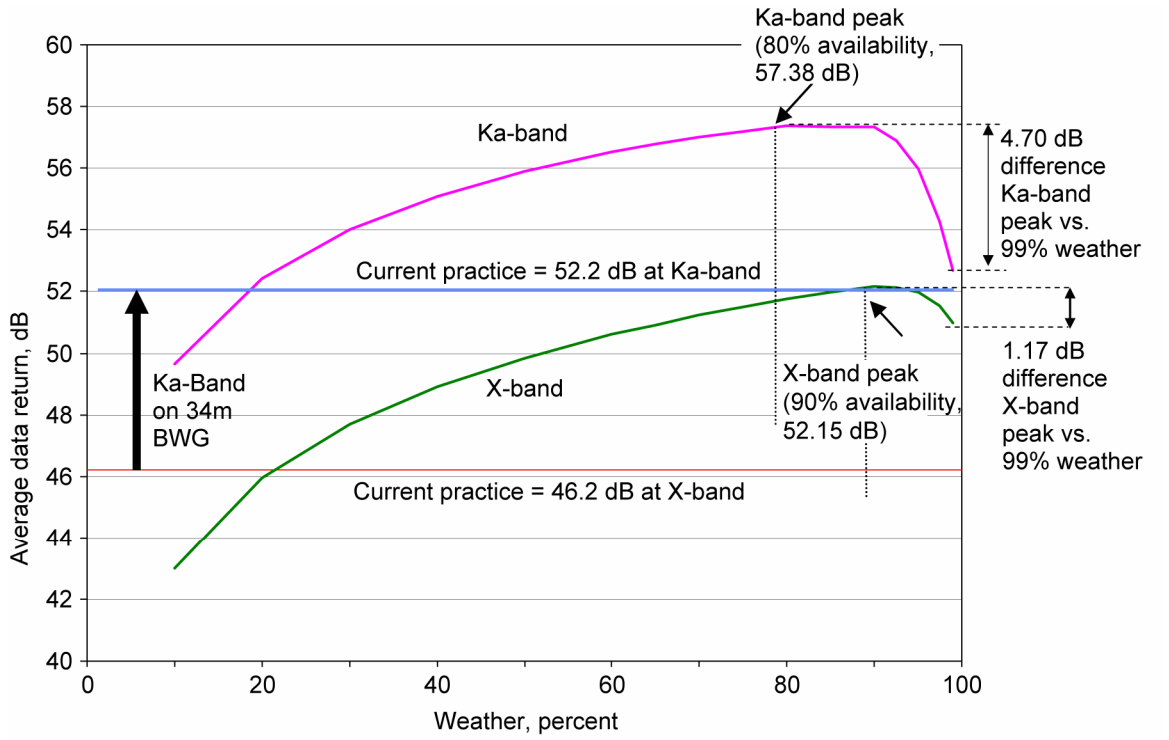

Figure 3–3.—Ka-band and X-band data return versus percent weather. CVDR average data return versus percent weather, Pass 030, Madrid, X-band, and Ka-band.

If the required availability is higher than 90 percent, the advantage of Ka-band decreases. Relative to the peaks, a required availability of 99 percent reduces volume at Ka-band by 4.7 dB and volume at X-band by 1.2 dB. The data volume advantage of Ka-band over X-band at 99 percent reliability—for these particular conditions at Madrid—is 1.7 dB.

Figure 3–3 show that atmospheric effects have a much larger impact on the Ka-band link than the X-band link. Besides accounting for the average effect on SNR ratio for each frequency band, it is necessary to account for the large variability at Ka-band due to weather.

Use of Ka-band also creates a need to look into accurate statistical weather forecasting along with optimized and multi-data-rate systems to optimize the data return, operating with as low a margin as possible to commensurate with the defined risk of data loss. For a state-of-the-art review of weather treatment on deep space Ka-band links, see reference 3–11.

3.4 Mars Solar Conjunction

Radio signals passing near the Sun are affected by solar conjunction due to increased numbers of intervening charged particles causing intensity scintillation (fades) and phase scintillation of the spacecraft signals, leading to significant degradation. Signals on their way to or from a ground network site pass near the Sun in a superior conjunction (spacecraft, Sun, and Earth nearly in a straight line, with the spacecraft (near Mars in this case) on the opposite side of the Sun from the Earth).

Solar effects on communication are often expressed in terms of the Sun-Earth-Mars (SEM) angle. As shown in figure 3–4, the SEM angle is nearly the angular separation between the direction from the station to the center of the Sun and the direction to the spacecraft around

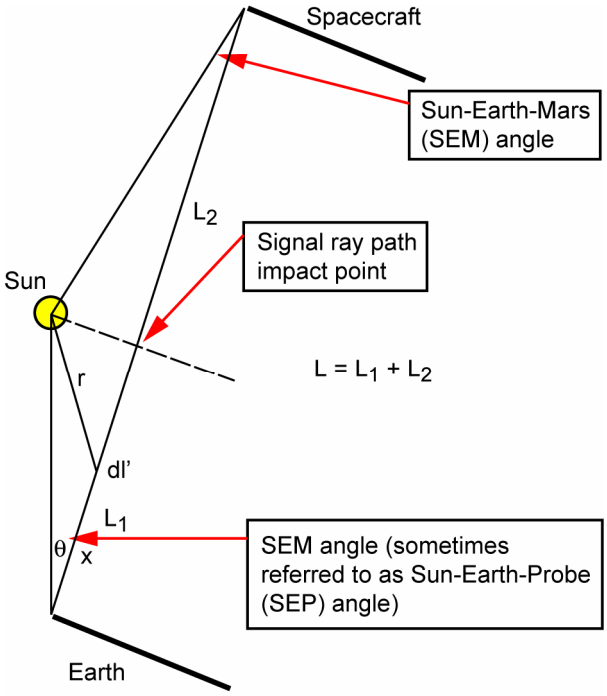

Figure 3–4.—Solar conjunction geometry at Mars.

Mars.[4] For the Mars-Earth link the visible solar disk has an average 0.26-deg radius as seen by the receiving antenna on the Earth.

The Earth-Mars distance is near its maximum during superior conjunction, resulting in minimum signal strength, independent of any solar effects.

As the SEM angle decreases, carrier locking and data detection issues become more stringent. The Sun affects a modulated carrier at Ka-band or X-band in several ways. Among these are spectral broadening, which causes an increase in the signal bandwidth due to electron density fluctuations and solar wind velocity; intensity scintillation and phase scintillation, which cause fading and Doppler noise; and system temperature increases at the station will be seen when the receiving antenna's side lobes intersect the solar disk.

From ref. 3–2, the Sun constantly produces the solar wind, consisting of turbulent ionized gases. These particles severely degrade the amplitude and phase of RF waves passing near the Sun through the turbulent regions. Additional degradation occurs during the portions of the 11-year solar cycle when coronal mass ejections and streamers become more frequent.

Figures 3–5 (for Ka-band) and 3–6 (for X-band) suggest, on average, that downlink performance becomes degraded at around 1° to 2° for Ka-band and around 2° to 3° for X-band (ref. 3–2). These data sets are based on observations from MGS in 1998 and Cassini in 2000. The MGS and Cassini spacecraft both use binary phase-shift keying (BPSK) modulation on the

[4]In solar conjunction studies, the general term Sun-Earth-Probe (SEP) angle is often used. Since this report deals only with spacecraft near Mars, the term Sun-Earth-Mars (SEM) angle is used. The Earth-Sun distance is much larger than the radius of the Earth and the Sun-Mars distance is much larger than the size of an aerostationary orbit around Mars. While the SEM angle is defined relative to the center of the Earth, it is very nearly the same as the Sun-station-orbiter angle. Reference 3–10 expresses geometry in terms of the solar radius (0.26° seen from Earth). An SEM angle of 0.26° is equivalent to one solar radius, and represents a signal skimming the edge of the visible solar disk.

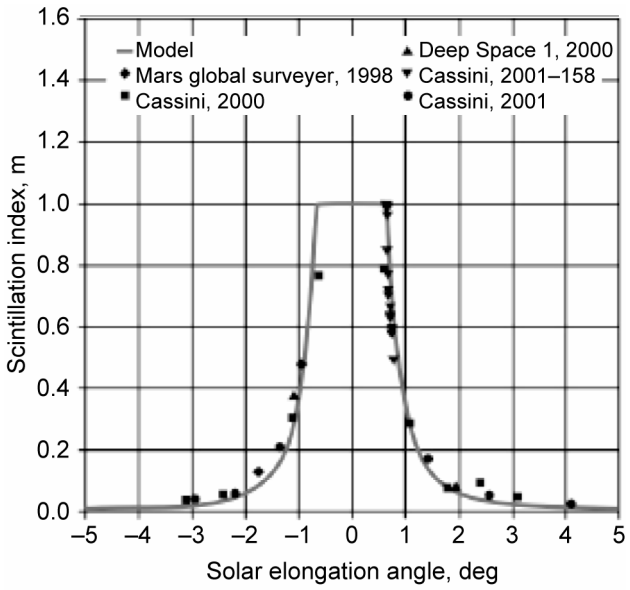

Figure 3–5.—Ka-band scintillation index as a function of SEM angle.

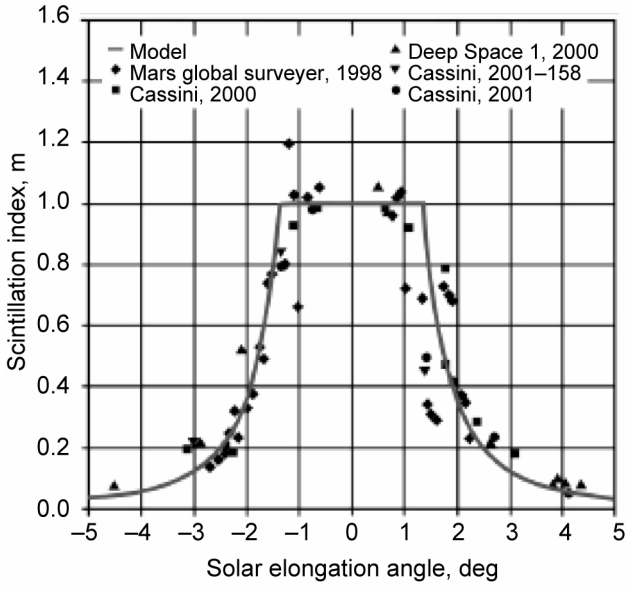

Figure 3–6.—X-band scintillation index as a function of SEM angle.

downlink carriers. For a given level of solar activity, Ka-band is less susceptible to the amplitude scintillation (fading) and spectral broadening effects of solar-charged particles than is X-band.

Table 3–5 shows the number of days of Mars solar conjunctions from 2010 to 2030 within bounds of 3°, 2°, 1°, 0.5°, and 0.4° SEM angle. Note that this table defines Ka-band in terms of a 1° SEM angle limit and X-band in terms of a 2° SEM angle limit for BPSK modulation. As described in (ref. 3–12), it becomes harder at Ka-band to maintain telemetry lock using phase-shift keying (PSK) modulation as the SEM angle decreases from 1° to 0.4°, the transition region between weak and strong scintillation.

TABLE 3–5.—DURATIONS OF Ka-BAND OR X-BAND OUTAGES FOR CONJUNCTIONS DURING 2010 TO 2030

Year	Days in which SEM angle is under:				
	3° (Optical)	2° (X-band BPSK)	1° (Ka-band BPSK)	0.5° (X/Ka-band FSK)	0.4° (Ka-band FSK)
2011	24.83	14.93			
2013	26.34	17.37	8.13	2.69	0.37
2015	21.42	13.88	5.73		
2017	17.9	10.71			
2019	16.92	10.17			
2021	17.8	11.49	4.61		
2023	19.85	13.22	6.57	3.22	2.53
2025	23.07	14.29	2.74		
2028	26.93	17.05	5.47		
2030	23.45	15.55	7.55	3.27	2.27
Total	218.5	138.7	40.8	9.2	5.2

As also shown in table 3–5, frequency shift keying (FSK) withstands close SEM angles better than PSK. Under weak signal conditions at small SEM angles, semaphores are expected to perform better even than FSK. (A semaphore is one frequency relative to carrier that is transmitted until some condition changes, at which time the frequency changes.) A second strategy during strong scintillation is the use of spatial diversity of receiving stations (separation of a few tens of km). A final challenge is to maintain communications when the signal ray path intersects the solar disk (SEM angle less than 0.26°).

From (ref. 3–13), robotic missions typically suspend or scale down their operations during periods centered on superior solar conjunctions. Such measures include invoking command moratoria, reducing tracking schedules, progressively lowering data rates, and minimizing onboard activities for a couple of weeks.

Human missions are likely to require continued communications through as much of the solar conjunction period as possible. For these, it may be necessary to consider various waveform options such as noncoherent FSK, semaphore-based communication, or to plan around the inevitable communication outage when BPSK is wiped out by solar effects.

Optical communication is generally not a substitute for radio communication at conjunction. For Earth-based optical receivers, looking directly into the Sun causes problems for sensitive optics. Discrimination of the optical signal in the presence of intense radiation—as well as thermal effects on the telescope—results in not being able to use optical communication for SEM angles less than 3°, limiting the number of days that optical communications would be available.

3.5 Spectrum (Ka-Band Frequency Allocations)

Mission Category Definitions

Category A: Maximum spacecraft-Earth range less than 2 million km

Category B (deep space): Maximum spacecraft-Earth range greater than 2 million km

Thus, a lunar or Earth-Moon L2 mission[5] is a Category A, and a Mars mission is a Category B.

Spectrum Allocations

Lunar and deep space missions, human and robotic, have different Ka-band frequency allocations. Table 3–6 defines the uplink (forward) and downlink (return) link allocations, as recommended by the Space Frequency Coordination Group (SFCG).

TABLE 3–6.—Ka-BAND FREQUENCY ALLOCATIONS

Mission category	Mission	Uplink (forward) band (GHz)	Downlink (return) band (GHz)
A	TDRSS	None	25.5 to 27.0
A	Lunar, L2; human and robotic (SFCG)	None	37.5 to 38.0
B	Deep space robotic exploration	34.2 to 34.7	31.8 to 32.3
B	Deep space human and robotic exploration (SFCG)*	40.0 to 40.5	37.0 to 37.5
* Includes deep space technology demonstration in near-Earth regions.			

3.6 The Challenge of Mars-Earth Distance Variation

The data rate that can be supported from Mars is a function of, among other things, the range between Earth and Mars. Figure 3–7 shows the fraction of time that the power needed to close a Mars link is a given dB value less than the power need at maximum distance. (The figure is derived from idealized assumptions of circular, coplanar orbits of Earth and Mars.)

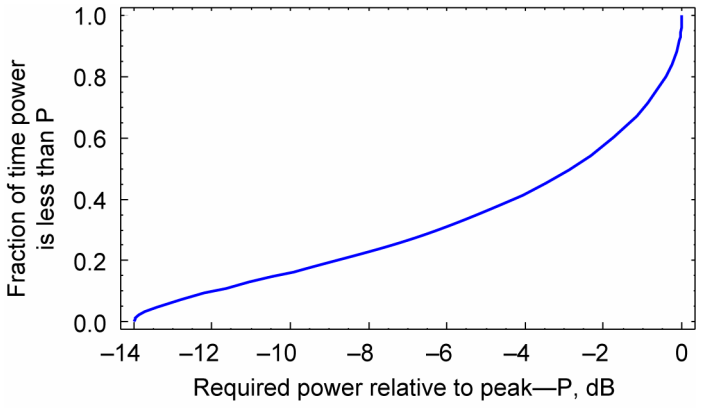

Figure 3–7.—Fractional time versus required power.

[5] The L2 point is a location roughly 1.4 million km in the anti-Sun direction from the Earth. A spacecraft at the L2 point will tend to follow the Earth as it goes around the Sun.

Approximately half of the time the Mars-Earth distance will be greater than 1.9 AU, which is 75 percent of the average maximum of 2.5 AU. There is a steep reduction in the required power (more than 10 dB) for the remaining half of the time.

Long-duration missions could take the communication performance difference due to distance into account when planning their missions, both to take advantage of the minimum range and to assure above-threshold operation at maximum range. For example, at shorter ranges, a mission might require use of fewer DSN-array elements for a given downlink rate, thereby incurring a smaller per-pass operations cost.

Mars missions that require a physical return of crew or payload to Earth are constrained to conclude their Mars surface operations near conjunction to minimize the liftoff energy required for the return flight. This implies that a Mars-Earth communications design sized for maximum range will be needed during the mission.

The effect of the Mars-Earth distance variation between 2010 and 2030 on the possible data rate is shown in figure 3–8. This figure is normalized for a minimum required rate of 10 Mbps at maximum distance. The resulting rate available half the time (the median rate) is 20 Mbps. The figure shows available rates of about 480 Mbps at minimum distance and indicates a gain of about 16.5 dB.

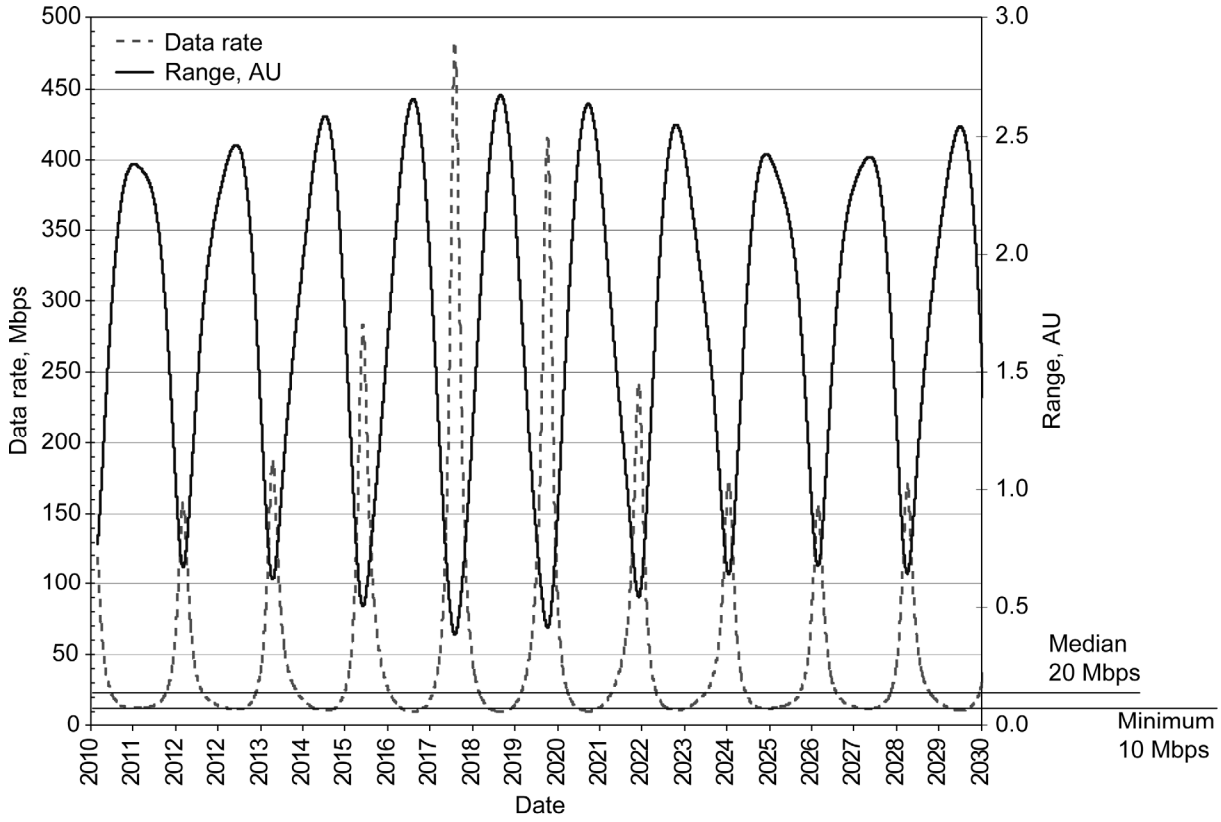

Figure 3–8.—Required power and range variation: Earth-Mars, 2010 to 2030.

3.7 References

3–1 Noreen, G., et al.: Mars Telecommunications Orbiter Ka-Band Operations., 9th Ka and Broadband Communications Conference, Lacco Ameno, Italy, Nov. 2003.

3–2 DSMS Telecommunications Link Design Handbook, TMOD No. 810–005, Rev. E, Jet Propulsion Laboratory, California Institute of Technology, Pasadena, CA, Jan. 2001. (This report contains information from module 101 (70-m subnet), module 103 (34-m HEF subnet), module 104 (34-m BWG subnet), module 105 (atmospheric effects), and module 106 (solar effects.)

3–3 Gatti, M.S.: The Deep Space Network Array. IEEE Microwaves and Theory and Techniques (MTT) Workshop on Arrays, June 17, 2005.

3–4 Statman, J., et al.: Deep Space Mission Systems (DSMS) Array Update, to JPL Executive Management Board, Jan. 18–19, 2005 (internal JPL document).

3–5 Gatti, M.S.: Private communication. Nov. 10, 2005.

3–6 Gatti, M.S.: The Deep Space Network Large Array. IPN Progress Report, vol. 42–157, pp. 1–9, May 15, 2004.

3–7 Harcke, L.J., et al.: Recent Ka-Band Weather Statistics for Goldstone and Madrid. TDA Progress Report, vol. 42–125, Jet Propulsion Laboratory, Pasadena, CA, May 1996.

3–8 Morabito, D.: Ka-Band Atmospheric Induced Temperature Fluctuations. IPN Progress Report, vol. 42–150, Jet Propulsion Laboratory, Pasadena CA, Aug. 2002.

3–9 Shambayati, S.: On the Benefits of Short-Term Weather Forecasting for Ka-Band. Aerospace, 2004.

3–10 Shambayati, S.: Maximization of Data Return at X-Band and Ka-Band on the DSN's 34-Meter Beam-Waveguide Antennas. TMO Progress Report, vol. 42–148, Jet Propulsion Laboratory, California Institute of Technology, Pasadena, CA, Feb. 2002.

3–11 Davarian, F., et al.: Deep Space Ka-Band Link Management and Mars Reconnaissance Orbiter: Long Term Weather Statistics Versus Forecasting. IEEE Proceedings, vol. 92 1879–1894, Dec. 2004.

3–12 Morabito, D. and Hastrup, R.: Communicating With Mars During Periods of Solar Conjunction. IPN Progress Report, vol. 42–147, Jet Propulsion Laboratory, Pasadena CA, Nov. 2001.

3–13 Noreen, G., et al.: Integrated Network Architecture for Sustained Human and Robotic Exploration. 2005 IEEE Aerospace Conference, Big Sky, MT, Mar. 5, 2005, updated Dec. 28, 2004.